EVALUATION OF THORACIC DEFLECTION CRITERIA IN FRONTAL COLLISION USING THORACIC IMPACTOR SIMULATION WITH HUMAN BODY FE MODEL

Takayuki Kawabuchi, Yasuhiro Dokko
Honda R&D Co., Ltd. Automobile R&D Center
Japan

Paper Number 19-0068

ABSTRACT

When involved in vehicle accidents, the fatality rate of thoracic injury is high, following head injury, and the major causality is a rise of organ injury rates due to an increase in the Number of Fractured Ribs (NFR). Previous studies suggested a high correlation between thoracic deflection and NFR. However, the correlation was evaluated primarily using test data in frontal collisions with restraint systems such as seatbelts or airbags. Thus, it was not evaluated by local loading. The objective of this paper is to evaluate the correlation between the thoracic deflection criteria and NFR under local loading conditions by thoracic impactor loading.

In order to evaluate the relationship between thoracic deflection criteria and NFR by localized loading, thoracic impact is more proper than sled impact, in which loading location and direction depend on restraint systems. Impact simulations were conducted on 19 points to cover the whole right side of the thorax. The simulations were conducted with the Global Human Body Model Consortium (GHBMC) 50th percentile male model for LS-DYNA. Deflection of each rib was measured at its anterior tip and Rmax was calculated using the deflections on the 4th rib and the 7th rib to represent Anthropometric Test Dummy (ATD) measurement points. In addition, Average Deflection of All Ribs (ADAR) and Weighted Average Deflection of All Ribs (WADAR) were calculated as proposed criteria. Then the correlation between NFR and each of those criteria was evaluated using the correlation coefficient.

The results showed that some specific impact points lower the correlation between NFR and Rmax. Impacts around 1st through 3rd ribs incur rib fractures without deflection on the representative points because the sternum and costal cartilage do not transmit the force and deflection to other ribs. On the other hand, ADAR showed a higher correlation with NFR than Rmax, and WADAR further improved correlation with NFR.

The results showed that WADAR needs to be taken into account to improve correlation between NFR and thoracic deflection. It suggests that deflection of all ribs modified by homogeneity of each rib deflection need to be considered in order to properly evaluate rib fractures caused by localized loadings.

The thoracic deflection criterion using weighted average deflection of all ribs showed the highest correlation with NFR and it allows evaluating rib fractures even under localized loading conditions.

INTRODUCTION

Thoracic fatal injuries sustained by seatbelt-restrained occupants in frontal crashes appeared to be as equally frequent as, or following, head fatal injuries [1]. Kent et al. described that the percentages of drivers who died with Maximum Abbreviated Injury Score (MAIS) related to rib fractures increased with aging and suggested that rib fracture was associated with the significantly increasing fatality rate of thoracic injuries, especially on elderly drivers [2]. In addition, approximately 47% of elderly drivers died due to fatal thoracic injuries, while 24% of younger drivers did [2]. Furthermore, it is estimated that the population of adults over 65 years old would increase up to 83.7 million by the year 2050 in the United States [3] and it would result in increasing number of drivers sustaining severe injury on the thorax in traffic accidents. Hence, the necessity of consideration for thoracic protection is growing more than ever.

Kent et al. suggested that the risk of rib fractures increased with the level of thoracic compression and that thoracic injury risk was often described by the antero-posterior deflection of the thorax [4]. Most of the correlation between thoracic deflection criteria and thoracic injury risk was evaluated primarily using test data by Anthropometric Test

Dummy (ATD) and Post Mortem Human Subjects (PMHS) in frontal collisions with restraint systems such as seatbelt and/or airbag. However, rib fractures may often be likely to occur not only by restraint systems but also by contact with interior components. Small overlap or oblique collisions cause oblique motion to occupants and the thorax has contact with deformed interior components [5] [6]. Such a loading condition differs from the loadings by restraint systems and it may rather be similar to some localized loading than a broad loading.

The objective of this study was to evaluate the correlation between the thoracic deflection criteria and the number of fractured ribs (NFR) under localized loading using thoracic impact simulations with various impact locations and directions using a human body model.

METHOD

Human Body Model

Global Human Body Models Consortium's 50th percentile male occupant model (GHBMC M50-O) v4.5 for LS-DYNA was adopted as a baseline model and was modified to have a thorax with elderly features for evaluation of thoracic deflection criteria. Rib fracture was predicted by elements exceeding the failure strain threshold, thus it was needed to validate the relationship between loading and strain on rib cortical bones. Single rib and rib cage of GHBMC M50-O was validated against the relationship between rib fracture and deformation under various boundary conditions [7]. As a validation for single rib, the relationship between rib deflection and strain of each rib was validated by an anterior to posterior bending test. [8] And as a validation for rib cage deformation, thoracic response against localized loading was validated by the point loading at various locations [9]. Based on those validations, the GHBMC M50-O model was considered to be able to evaluate rib fractures caused by localized loadings at various points.

The representative age for the elderly was set at 75 years old based on Ito et al [10]. The material properties of rib cortical bone for the baseline model was modeled with piecewise linear plasticity material model with Young's modulus, yield stress, and a failure strain. The Young's modulus of the rib cortical bone was set at 11.5 MPa and yield stress was set at 88 MPa based on Li et al [11]. Failure strain was determined by the sum of yield strain and ultimate plastic strain. Yield strain was 0.0077, which was calculated by Young's modulus and yield stress. The ultimate plastic strain of the cortical bone had correlation with age as given in Equation 1 [12] and set at 0.0088. Thus, the failure total strain as a rib fracture threshold resulted in 1.65% and shell elements constituting rib cortical bone model were judged as a fracture when the strain on an element exceeds the threshold.

$$\text{Ultimate plastic strain [unitless]} = \frac{-383age[years] + 37514}{10^6} \qquad \text{(Equation 1)}$$

Rib cortical bone thickness was decreased from the baseline model based on the aging function of linear relationship between age and rib cortical bone thickness described by Ito et al [10]. Since the base age of GHBMC M50-O was not explicitly defined, it was assumed average, and the cortical bone thickness at 75 years old was presumed. Rib cortical bone thickness of GHBMC M50-O v4.5 was distributed on every shell element of the rib derived from CT scan data and its average thickness was 0.67 mm [8]. Thereby base age was assumed as roughly 60 years old and was decreased based on the aging function. The Young's modulus of the costal cartilage was set at 19.7 MPa based on Yamada [13]. Kent et al. showed upward geometrical change by aging and described those changes on rib cage influences on increasing stiffness of rib cage [14]. On the other hand, Ito et al compared the contribution of thorax characteristic change by aging and showed that the influence of the geometrical change of rib cage was smaller than change of cortical bone thickness or failure strain [15]. In addition, the aim of this study was to evaluate the relationship between rib cage deformation and NFR on same subject. Therefore, the authors decided that the rib cage geometry was not to be modified in this study. The model with those modifications was validated against frontal thorax impact tests and belted full body frontal sled tests [16].

Thoracic impact simulation

Thoracic impactor loading was conducted in order to represent localized loading and reconstruct thoracic deformation due to a localized loading by interior components such as door trims. Besides, the thoracic impactor was presumed to be able to comprehensively evaluate the relationship between thoracic deflection criteria and NFR since the impactor did not depend on the character of restraint systems.

A rigid impactor model with a small diameter was employed in order to generate localized loading on the thorax. The impactor was a cylindrical shape with a 75 mm diameter and its mass was 22 kg. The initial velocity was set at high and low velocity along the axis direction of the impactor, 6.7 m/s and 4.7 m/s respectively as boundary conditions. Low velocity was determined to be a half of the kinetic energy of high velocity in order to evaluate velocity dependence of the relationship between rib fracture and thorax deflection. Centers of impactor contact locations were set at 19 points on the whole right half of the thorax. The impact region was focused on the single side based on the assumption that the rib cage was symmetrical. A base contact point was set to match the center of the impactor on a point on the sternum 70 mm superior to the tip of the xiphoid. The point was approximately the same height as the 4th rib. The impact direction was determined to be perpendicular to the plane on the thoracic surface, which was defined as 63.5 degrees to the horizontal plane and depicted as Figure 1. The other 18 contact points were set on each place with each direction described in Table 1 and Figure 1. Each contact point was set at a point on position Y and Z defined as lateral and vertical coordinates from the base contact point. The impact direction seen from the impactor side view was same as that of base contact point. The Z angle shown in Figure 1, which defines an angle of the impactor around vertical axis, was set to be perpendicular to the thoracic surface and angles at each point were shown in Table 1.

Table 1.
Impactor contact positions

Point No.	Position Z [mm]	Position Y [mm]	Angle Z [deg]
1	0	0	0
2	125	0	0
3	125	75	30
4	125	125	50
5	75	0	0
6	75	75	20
7	75	125	50
8	75	150	60
9	0	75	20
10	0	125	40
11	0	150	65
12	-75	0	0
13	-75	75	20
14	-75	125	40
15	-75	150	60
16	-150	0	0
17	-150	75	20
18	-150	125	40
19	-150	150	60

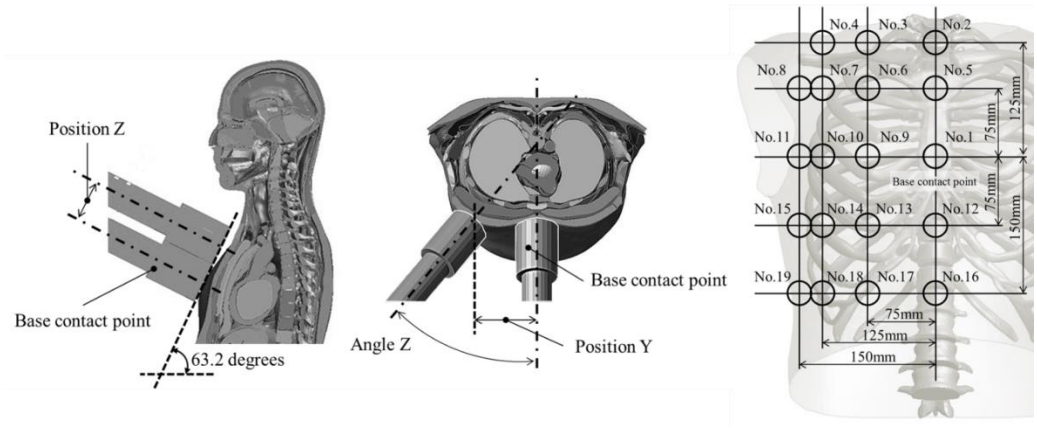

Figure 1. The definition of parameters and impact positions

Rib Deflection Measurement

Rib deflection in X, Y, and Z (XYZ) directions was measured at each rib anterior tip. The local coordinate system was defined at the costovertebral joint of each rib. The local x axis pointed anterior direction of the thorax, the local y axis pointed right-hand direction and the local z axis pointed upward. Since rib deformation caused by oblique loading was largely related to y deflection, resultant deflection was applied to criteria. Measurement results were processed and defined as a criterion and the correlation between the criteria and NFR were evaluated by the correlation coefficient defined as the R-squared values (R^2), which were calculated by linearization.

Rib deflection evaluation criterion

Two types of criteria were defined for rib deflection evaluation. One type was using a value of the largest deflection between all ribs and the other type was using an average value of normalized all rib deflections.

A. **Criterion using the largest rib deflection:** The criterion defined the larger one of maximum XYZ resultant deflections of the 4th Rib and the 7th Rib as a representative point. The representative ribs were determined to be similar to the measurement points of Infra-Red Telescoping Rod for the Assessment of Chest Compression (IR-TRACC) applied to Test device for Human Occupant Restraint (THOR) ATD. This criterion was defined as Rmax.

Furthermore, the largest one between the maximum XYZ resultant deflections of the 12 ribs was defined as a criterion. This was defined as Maximum Deflection of All Ribs (MDAR).

B. Criterion using average value of normalized all rib deflections: For a comparison with the criteria using maximum value, average value of the maximum XYZ resultant deflection of the 12 ribs was defined as a criterion. The amount of deflection to fracture is different among every rib since they have different shapes and lengths. Those differences should be taken into account to evaluate NFR by an average deflection of the 12 ribs. In order to remove the influences of that, each XYZ resultant deflection was normalized by initial length between a measurement point and the coordination origin of each rib. The definition of initial length and length of each rib were depicted in Figure 2 and Table 2, respectively. The criterion was defined as Average Deflection of All Ribs (ADAR) and given in Equation 2.

$$\mathrm{ADAR} = \frac{\sum_{i=1}^{n}(d_i/L_i)}{n} \qquad \text{(Equation 2)}$$

Where, di = normalized deflection of each rib

Li = rib initial length

n = Number of ribs. Here this is 12.

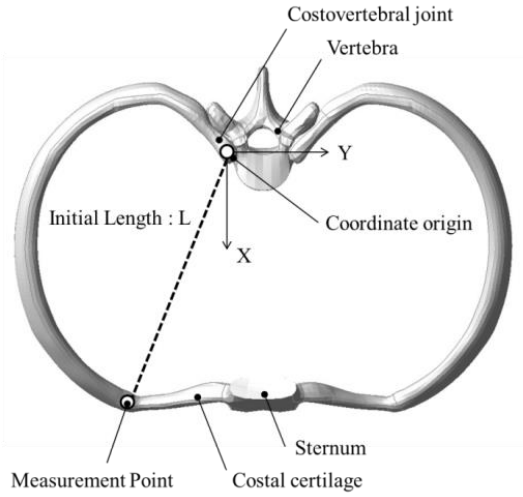

Figure 2. Rib measurement point and detail of the location

Table 2.
Initial length of each rib

Rib No.	Initial Length L [mm]
1	73.7
2	108.6
3	145.0
4	173.0
5	189.4
6	199.7
7	204.1
8	208.9
9	198.2
10	176.8
11	151.4
12	94.6

RESULTS

All results of evaluation criteria and NFR of each impact point were listed on Table A1 and Table A2.

The relationships between Rmax, MDAR, and NFR were shown in Figure 3(a) and 3(b). R^2 of Rmax was lower than that of MDAR. This is assumed because NFR were varied from 0 to 6 between Rmax 20 mm and 30 mm, while such a variance did not happen for MDAR. The relationship between ADAR and NFR was shown in Figure 3(c). The R^2 was higher than Rmax or MDAR and the scatter became smaller.

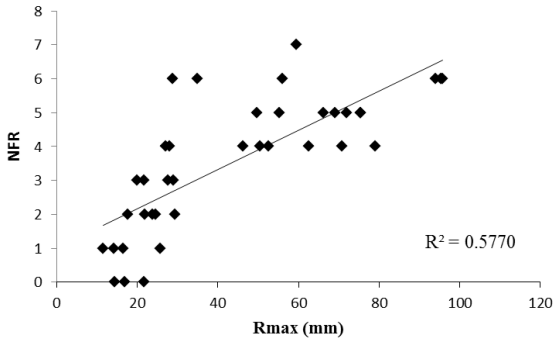

(a) Rmax vs NFR

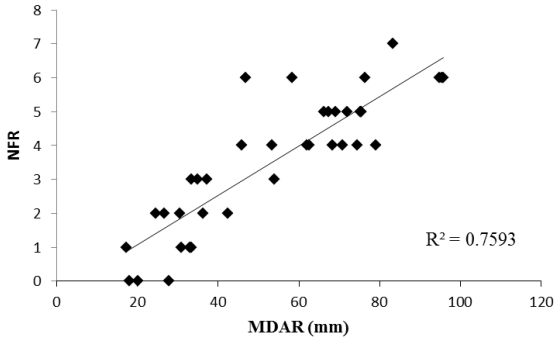

(b) MDAR vs NFR

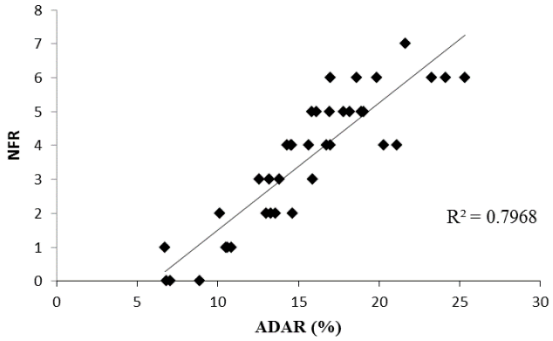

(c) ADAR vs NFR

Figure 3. Correlations between rib deflection criteria and NFR

However, some deformation patterns, which were provided in Figure 4(a) and 4(b), showed large different NFR even under the same ADAR. The impact point at No.6 incurred 4 fractured ribs while No.14 incurred 7 fractured ribs. It found that the difference of deformation shape affected NFR.

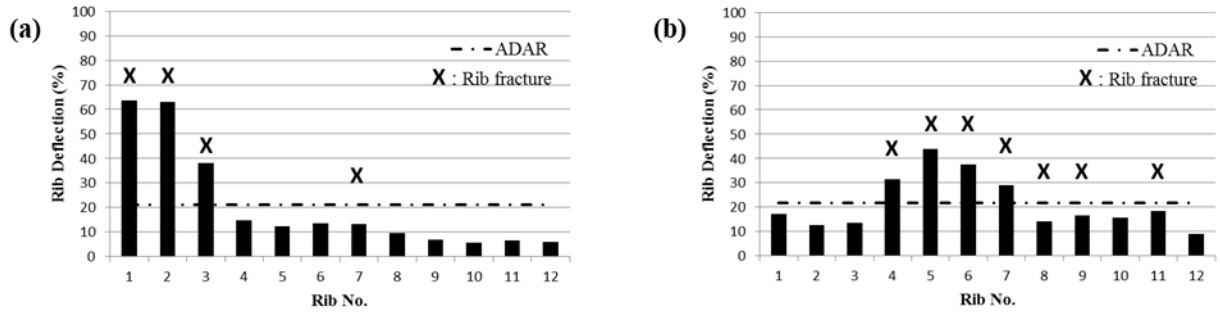

Figure 4. Each rib deflection: (a) at impact point No.6 and (b) at impact point No.14

Thus, a weighting factor was applied to ADAR in order to distinguish the deformation shape due to effects of impact point differences. Edwards et al suggested evaluating a degree of deformation of deformable barrier by homogeneity of deformation [17]. Based on this evaluation method, homogeneity of thoracic deformation shape was applied to a criterion adopting a weighting factor. The criterion was defined as Weighted Average Deflection of All Ribs (WADAR) as described in Equation 3. The weighting factor is the parentheses in the equation. The second term of the weighting factor, which indicates inhomogeneity, becomes large when the local deformation occurs largely on the thorax. In other words, the degree of local deformation, which has large ADAR and small NFR, is larger and WADAR becomes smaller. This weighting factor adjusts the inconsistency between ADAR and NFR as described above.

$$\mathrm{WADAR} = \left(0.2 - \frac{\sqrt{\sum_{i=1}^{n}(ADAR - d_i)^2}}{n}\right) \times ADAR \qquad \text{(Equation 3)}$$

Where, di = normalized deflection of each rib

n = number of ribs. Here, this is 12.

Further, the first term, 0.2, was empirically determined to make a correlation coefficient higher.

Figure 5 shows the relationships between WADAR and NFR. R^2 of WADAR is higher than that of ADAR. WADAR of No.6 and No.14 were 2.97% and 3.66%, respectively and they showed the differences although their ADAR was almost the same.

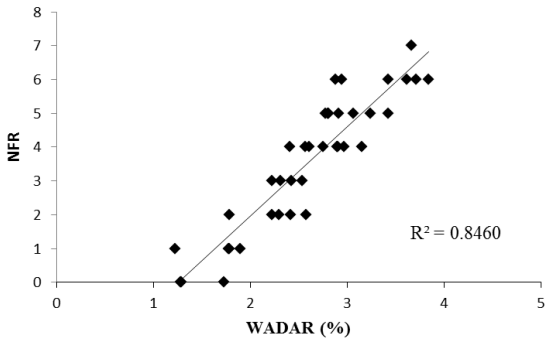

Figure 5. Correlation between WADAR and NFR

DISCUSSION

As mentioned above, WADAR indicated the highest R^2 between four criteria. Considering the fracture mechanisms, impact energy generated by a thorax impactor incurs thoracic deformation and rib fracture occurs when it becomes beyond the critical value. When larger energy is applied, NFR will increase. Since WADAR is based on ADAR, using the sum of all rib deflections as shown in Equation 2, it had a better correlation with NFR than those of criteria using maximum deflections as a representation. Impact on the upper region of the thorax concentrates the energy on one or a few neighboring ribs and incurs rib fractures around that limited region. Under such a condition, NFR increased without deformation at the representative point when remote region from representative points, such as around clavicle or upper part of rib cage, were impacted. Costal cartilage around the sternum deforms largely and just transmits little rib deformation to the 4th rib or the 7th rib, which was defined as a representative point for THOR's IR-TRACC. These results may suggest that the criterion using the deformation of representative points possibly has low sensitivity to evaluate rib fracture injury under localized loading conditions.

As indicated in Figure 4, large localized deformation of the thorax increases the average of rib deflection without NFR increase and results in overestimation of ADAR with R^2 reduction. This result indicates the necessity to distinguish deformation shape for NFR prediction. WADAR is possible to modify such overestimated ADAR by distinguishing such localized deformation from uniform deformation by a weighting factor. A weighting factor evaluates homogeneity of rib cage deformation shape. The weighting factors of the impact points at No.6 and No.14 were 0.141 and 0.169, respectively. As such, the value of the weighting factor is small for local deformation. The weighting factor modified overestimated ADAR, which shows large value although the NFR is small. Those modifications for distinguishing deformation patterns represented improvement of a correlation between the criterion and NFR.

This study proposed the criterion indicating high correlation with NFR. As future work, the accuracy and robustness should be improved in order for evaluation under same conditions as actual accidents with interior component and restraint systems, such as seatbelts and/or airbags. The criterion is currently based on the results under impact on a single side, thus, it should be improved to evaluate including the non-impacted side. Since this study did not show the physical meaning of coefficient in WADAR, the meaning of value should be considered in a future work.

In addition, the criterion was applied to only the human body, while the manner to apply to ATD should be considered. The THOR dummy is limited in evaluation for frontal collision mode and the thoracic deformation measurement device is currently only four IR-TRACCs. The alternative methods for these limitations should be considered to apply WADAR to the THOR dummy.

CONCLUSIONS

The thoracic deflection criterion using weighted average deflection of all ribs showed the highest correlation with NFR and it allows evaluating rib fractures even under localized loading conditions. Distinguishing deformation patterns improved the prediction of NFR by rib deflections. That suggested that the criterion using the deformation of representative points has possibly low sensitivity to evaluate rib fracture injury under localized loading conditions.

It is not possible to evaluate deflections of all ribs with the current ATD, thus a method to measure all rib deflections, or another alternative, is needed.

REFERENCES

[1] Kent, R.W., Henary, B., Matsuoka, F., 2005. "On the fatal crash experience of older drivers." Annu Proc Assoc Adv Automot Med. 49: 371–391.

[2] Kent, R.W., Woods, W., Bostrom, O., 2008. "Fatality risk and the presence of rib fractures." Ann Adv Automot Med. 52: 73–84.

[3] National Highway Traffic Safety Administration. 2017. "Traffic Safety Facts 2015." DOT HS 812 372, 1-5, Available at https://crashstats.nhtsa.dot.gov/#/DocumentTypeList/12. Accessed November 22, 2018

[4] Kent, R.W., Patrie, J., Poteau, F., 2003. "Development of an age-dependent thoracic injury criterion for frontal impact restrain loading." Proc. Int. Tech. Conf. Enhanced Safety Vehicles 2003; 12

[5] Iraeus, J., Lindquist, M., 2013. "Evaluation of chest injury mechanisms in nearside oblique frontal impacts." Ann Adv Automot Med. Sep; 57: 183–196.

[6] Brumbelow, M.L., Farmer, C.M., 2013. "Real-world injury patterns associated with hybrid III sternal deflections in frontal crash tests." Traffic Injury Prevention, vol. 14, issue 8

[7] Global Human Body Models Consortium, Available at http://www.ghbmc.com/publication/

[8] Li, Z., Subit, D., Kindig, M., Kent, R., 2010, "Development of a Finite Element Ribcage Model of the 50th percentile Male with Variable Rib Cortical Thickness." 38th International Workshop on Human Subjects for Biomechanical Research, National Highway Traffic Safety Administration, U.S. D.O.T.

[9] Poulard, D., Subit, D., 2015. "Unveiling the Structural Response of the Ribcage: Contribution of the Intercostal Muscles to the Thoracic Mechanical Response." Proc. Int. Tech. Conf. Enhanced Safety Vehicles 2015

[10] Ito, O., Dokko, Y., Ohashi, K., 2009. "Development of adult and elderly FE thorax skeletal models." SAE Technical Paper 2009-01-0381

[11] Li, Z., Kindig, M.W., Kerrigan, J.R., Untaroiu, C.D., Subit, D., Crandall, J.R., Kent, R.W., 2010. "Rib fractures under anterior–posterior dynamic loads: Experimental and finite-element study." Journal of Biomechanics, vol. 43, issue 2, 228 - 234

[12] Schoell, S.L., Weaver, A.A., Vavalle, N.A., Stitzel, J.D., 2015, "Age- and sex-specific thorax finite element model Development and Simulation." Traffic Injury Prevention, vol. 16, issue sup1

[13] Yamada, H., 1970. "Strength of biological materials." Williams & Wilkins

[14] Kent, R.W., Lee, S., Darvish, K., Wang, S., Poster, C.S., Lange, A.W., Brede, C., Lange, D., Matsuoka, F., 2005. “Structural and Material Changes in the Aging Thorax and Their Role in Crash Protection for Older Occupants.” Stapp Car Crash Journal, vol.49, 231-249

[15] Ito, O., Ito, Y., Dokko, Y., Mori, F., Ohhashi, K., 2010. “Successive development of adult and elderly FE thorax models (Japanese).” Paper presented at: Society of Automotive Engineers of Japan (JSAE), paper #20105713

[16] Kawabuchi, T., Takahashi, Y., 2018. “Verification of rib fracture prediction in frontal collision.” Paper presented at: International Research Council on Biomechanics of Injury (IRCOBI); September 12-14, 2018; Athens, Greece

[17] Edwards, M., Davis, H., Hobbs, A., Thompson, A., 2003. “Development of test procedures and performance criteria to improve compatibility in car frontal collisions.” Proceedings of the Institution of Mechanical Engineers Part D Journal of Automobile Engineering, 2003

APPENDIX A

Table A1.

Table of value of criteria at impactor speed 6.7m/s

Impact point No.	NFR	Rmax [mm]	MDAR [mm]	ADAR [%]	WADAR [%]
1	2	29.3	36.3	13.6	2.42
2	1	14.3	17.4	6.7	1.22
3	2	21.8	42.4	14.6	2.30
4	2	24.6	30.5	13.0	2.23
5	3	19.9	37.3	13.8	2.31
6	4	27.0	68.3	21.1	2.97
7	6	28.9	58.3	18.6	2.94
8	6	34.9	46.8	17.0	2.88
9	6	95.8	95.8	25.3	3.84
10	6	95.4	95.4	24.1	3.71
11	6	94.1	94.8	23.3	3.62
12	3	29.0	35.0	13.2	2.54
13	5	55.4	75.3	18.9	3.24
14	7	59.5	83.3	21.6	3.66
15	6	56.1	76.4	19.9	3.42
16	2	23.9	26.7	13.3	2.57
17	5	69.1	69.1	19.1	3.42
18	5	75.4	75.4	17.8	3.07
19	4	70.8	70.8	16.7	2.90

Table A2.

Table of value of criteria at impactor speed 4.7m/s

Impact point No.	NFR	Rmax [mm]	MDAR [mm]	ADAR [%]	WADAR [%]
1	1	25.7	31.0	10.6	2.42
2	0	14.5	18.1	7.1	1.22
3	1	16.5	33.1	10.8	2.30
4	2	17.7	24.5	10.1	2.23
5	1	11.5	33.5	10.5	2.31
6	3	21.7	54.0	15.9	2.97
7	4	28.0	45.8	14.6	2.94
8	3	27.7	33.5	12.6	2.88
9	4	79.1	79.1	20.3	3.84
10	5	75.4	75.4	18.2	3.71
11	5	71.9	71.9	16.9	3.62
12	0	21.8	27.9	6.8	2.54
13	4	46.3	62.0	15.7	3.24
14	4	50.6	74.5	17.0	3.66
15	5	49.8	67.4	16.1	3.42
16	0	16.9	20.2	8.9	2.57
17	4	52.6	53.3	14.3	3.42
18	5	66.2	66.2	15.8	3.07
19	4	62.6	62.6	14.5	2.90